

# Semantic Classification of Urban Trees Using Very High Resolution Satellite Imagery

Dawei Wen, Xin Huang, *Senior Member, IEEE*, Hui Liu, Wenzhi Liao, *Member, IEEE*,  
and Liangpei Zhang, *Senior Member, IEEE*

**Abstract**—There is an urgent need for urban tree classification, in order to assist with ecological environment protection and provide sustainable development guidance for urban planners. While most of the existing studies have concentrated on tree crown extraction or tree species identification, only a few studies have attempted to conduct semantic classification of urban trees from an urban habitat perspective. The lack of semantic information means that it is difficult to meet the needs of ecological and environmental issues. As such, in this study, a novel three-level (pixel-object-patch) framework for semantic classification of urban trees is proposed to categorize urban trees as park, roadside, and residential-institutional trees. These three categories are cognized and conceptualized by humans and serve as different ecological functions in urban areas. Park is important urban greenery accommodated within recreational and cultural facilities. Roadside and residential-institutional trees are distributed along streets or in neighborhoods. The framework for the semantic classification of urban trees includes the following steps: 1) vegetation information extraction at the pixel level utilizing a spectral vegetation index; 2) vegetation-type classification at the object level employing spectral and textural features; and 3) urban tree classification at the patch level, where a series of metrics related to area, shape, structure, and spatial relationship are considered. Two typical Chinese megacities, Shenzhen and Wuhan, were chosen to demonstrate the applicability and effectiveness of the proposed method. The results reveal that the proposed method can achieve a satisfactory performance, with the overall accuracy reaching 85%. Moreover, the producer's and user's accuracies are generally high for most tree categories (>80%). The further landscape analysis demonstrates some general characteristics of the natural landscape configuration: residential-institutional trees show greater fragmentation and spatial heterogeneity, and park trees show the maximum physical connectedness and aggregation.

**Index Terms**—Natural landscape, semantic classification, trees, urban, very high resolution.

## I. INTRODUCTION

TREES, which are a dominant component of the urban natural landscape, play an important role in improving the urban ecological environment, through air filtration, microclimate regulation, noise reduction, and water quality amelioration [1]. In addition, there is evidence that urban trees can help to enhance public health [2] and lessen criminal behavior [3]. Therefore, inventorying the spatial distribution and detailed information (e.g., species and habitat types) of urban trees is imperative in decision-making about natural landscape management and planning [4], [5].

In general, the detailed classification of urban trees can be conducted via ground surveys, aerial photography, or remote sensing interpretation. However, conventional ground surveys can be cost- and time-intensive due to the urban scene complexity, landscape dynamics, and accessibility constraints for private areas [6], while the direct observation of land cover through aerial photography or satellite data can enable cost-effective tree classification. Aerial photographs have been the primary data source for the detailed classification of urban trees in previous research [7]–[9]. However, remote sensing satellites can now acquire data that span temporal and spatial scales with more spectral information in a more convenient way [10], [11]. These characteristics of remote sensing data have allowed tree classification at local [12]–[14], regional [15]–[17], and global [18], [19] scales. Most of these studies, however, have concentrated on estimating the vegetation extent at a rough scale using coarse- or moderate-resolution data, and they have neglected the detailed identification of individual tree crowns. Fortunately, very high resolution (VHR) remote sensing data have shown great potential in detailed urban classification [20], [21], and can be utilized to extract both the locations and the corresponding attributes (e.g., crown size and species) of individual trees. Markov random field based super-resolution mapping [22], fuzzy logic approaches [5], object-based approaches [23], and multisensor techniques [24] have all been applied for tree crown extraction. Moreover, urban tree species can be classified by fully exploiting the spectral and structural information contained in satellite data [14], [25]–[27].

Summarizing the existing literature, studies related to tree mapping have covered subjects spanning tree canopy extraction

Manuscript received July 3, 2016; revised October 10, 2016 and November 27, 2016; accepted December 14, 2016. This work was supported by the National Key Research and Development Program of China under Grant 2016YFB0501403, by China Science Fund for Excellent Young Scholars under Grant 41522110, and by the Foundation for the Author of National Excellent Doctoral Dissertation of PR China (FANEDD) under Grant 201348. (Corresponding author: Xin Huang.)

X. Huang is with the School of Remote Sensing and Information Engineering, Wuhan University, Wuhan 430079, China (e-mail: xhuang@whu.edu.cn).

D. Wen, H. Liu, and L. Zhang are with the State Key Laboratory of Information Engineering in Surveying, Mapping and Remote Sensing Wuhan University, Wuhan 430079, China.

W. Liao is with the Image Processing and Interpretation, Department of Telecommunications and Information Processing, Ghent University, 9000 Ghent, Belgium.

Color versions of one or more of the figures in this paper are available online at <http://ieeexplore.ieee.org>.

Digital Object Identifier 10.1109/JSTARS.2016.2645798

to tree species identification. However, the semantic analysis of urban trees remains a large gap to be filled. From an urban habitat perspective, the varied spatial patterns and ecological functions of trees allow them to be classified into three main habitat types: park, roadside, and residential–institutional trees [28]. Trees have been grown to serve various ecological and landscape functions in the urban environment. Urban parks serve many functions, such as providing social services, nurturing wildlife, and promoting city sustainability. Roadside trees can screen against noise, absorb vehicle emissions, and capture particulate matter [29], [30]. Trees in residential and institutional areas help to improve the quality of life for city dwellers [31]. Moreover, these three urban habitat types vary significantly in species composition, species diversity, and structure, and different policy and management strategies are warranted [32], [33]. Although the importance of habitat type (i.e., park, roadside, and residential–institutional trees) is widely acknowledged, only a few studies have focused on this aspect. Jim [34] detailed the formation and changes of the different urban habitat types during the urbanization process. Beyond this, the tree species and dimensions (i.e., the number of trees and the size of the tree crown) in the three habitat types have also been analyzed [28], [32], [33]. However, these studies remain at the stage of conceptual definition, or they employed predefined habitat information obtained by field survey and manual interpretation.

In this regard, we aim to conduct semantic classification of urban trees (i.e., park, roadside, and residential–institutional trees) using VHR remotely sensed imagery. These categories of urban trees are cognized and conceptualized by humans and serve as different ecological functions in urban areas. In our study, a three-level (pixel-object-patch) framework exploiting the spatial pattern variance (e.g., size, shape, structure, and spatial relationship) in park, roadside, and residential–institutional trees is proposed. At the pixel level, an effective vegetation index that is suitable for high-resolution remote sensing data is proposed in order to mask out nonvegetation areas, reducing the computational burden. The masked images are then fed into an object-based image analysis process, generating an accurate map of tree and ground vegetation. Subsequently, above the object-level result, a series of metrics describing the spatial patterns at the patch level (i.e., the aggregation of connected vegetation objects) are employed to categorize the three urban habitat types.

The rest of this paper is organized as follows. Section II presents the study areas and data sets. Section III details the proposed framework for tree-type mapping. In Section IV, the performance and accuracy of the obtained results are examined and analyzed. A discussion is provided in Section V. Finally, the conclusion is made in Section VI.

## II. STUDY AREA AND DATA SETS

In this study, the urban areas of two typical cities in China, i.e., Shenzhen and Wuhan, were chosen. Shenzhen, which is located in southern coastal China, is one of the most developed megacities in China. This region shows a typical subtropical climate, with an annual average temperature of 22.4 °C and

annual precipitation of 1933.33 mm. In Shenzhen, the vegetation type is representative of subtropical evergreen monsoon forest, and mainly consists of evergreen broad-leaved forest, coniferous forest, bamboo forest, shrubs, and grassland [35]. Wuhan, which is located in the middle-lower Yangtze Plain, is the largest city in Central China. Wuhan is situated in the subtropical monsoon climate zone, with four distinctive seasons. The annual temperature ranges from 15.8 °C to 17.5 °C and the annual average precipitation is 1269 mm. In addition, with regard to the vegetation type, subtropical evergreen broadleaf vegetation and temperate deciduous broadleaf vegetation are the dominant vegetation types in this area [36].

In our study, WorldView-2 imagery was used for the urban tree classification, the resolution of which was 2 and 0.5 m for the multispectral and panchromatic modes, respectively. In the image preprocessing steps, the quick atmospheric correction algorithm and image registration based on polynomial wrapping and nearest neighbor resampling were adopted. For the geometric accuracy, the root-mean-square error was 0.49 pixels. Subsequently, the Gram–Schmidt spectral sharpening technique followed by data downsampling was adopted to derive a pan-sharpened 8-band image with a spatial resolution of 1.0 m. The downsampling was undertaken to decrease the data volume, considering that the spatial resolution of 1.0 m is fine enough for categorizing tree types. In addition to the remote sensing satellite imagery, road information generated from openstreetmap (OSM) was employed as ancillary data. The study areas of Shenzhen and Wuhan are shown in Fig. 1(a) and (b), corresponding to  $10529 \times 7536$  (79.35 km<sup>2</sup>) and  $7190 \times 7893$  (56.75 km<sup>2</sup>) pixels, respectively.

## III. METHODOLOGY

From the urban habitat perspective, trees can be categorized as park, roadside, and residential–institutional (the left column of Fig. 2) [28]. The three tree categories show different appearance styles (referring to geometric features), which can be manifested as groups of interlocking trees, tree corridors, tree networks, or single trees (the middle column of Fig. 2). These appearance style differences can serve as the basis for identifying urban tree types. Specifically, the three urban tree categories can be described from the aspects of size, shape, structure, and spatial relationship, using remote sensing and GIS data (the right section of Fig. 2).

Based on the above-mentioned analysis, the proposed tree-type classification is conducted at three levels, i.e., pixel, object, and patch, as shown in Fig. 3. The workflow for the proposed tree-type classification is presented in Fig. 4. First, the vegetation is extracted using a vegetation index at the pixel level. Subsequently, the vegetation extraction result is fed into the object level as the mask layer. At the object level, a supervised method based on object-specific spectral and textural features is adopted to generate an accurate vegetation-type map (i.e., a map of the trees and ground vegetation). Finally, patch-level metrics are considered to differentiate the three tree types: park, roadside, and residential–institutional.

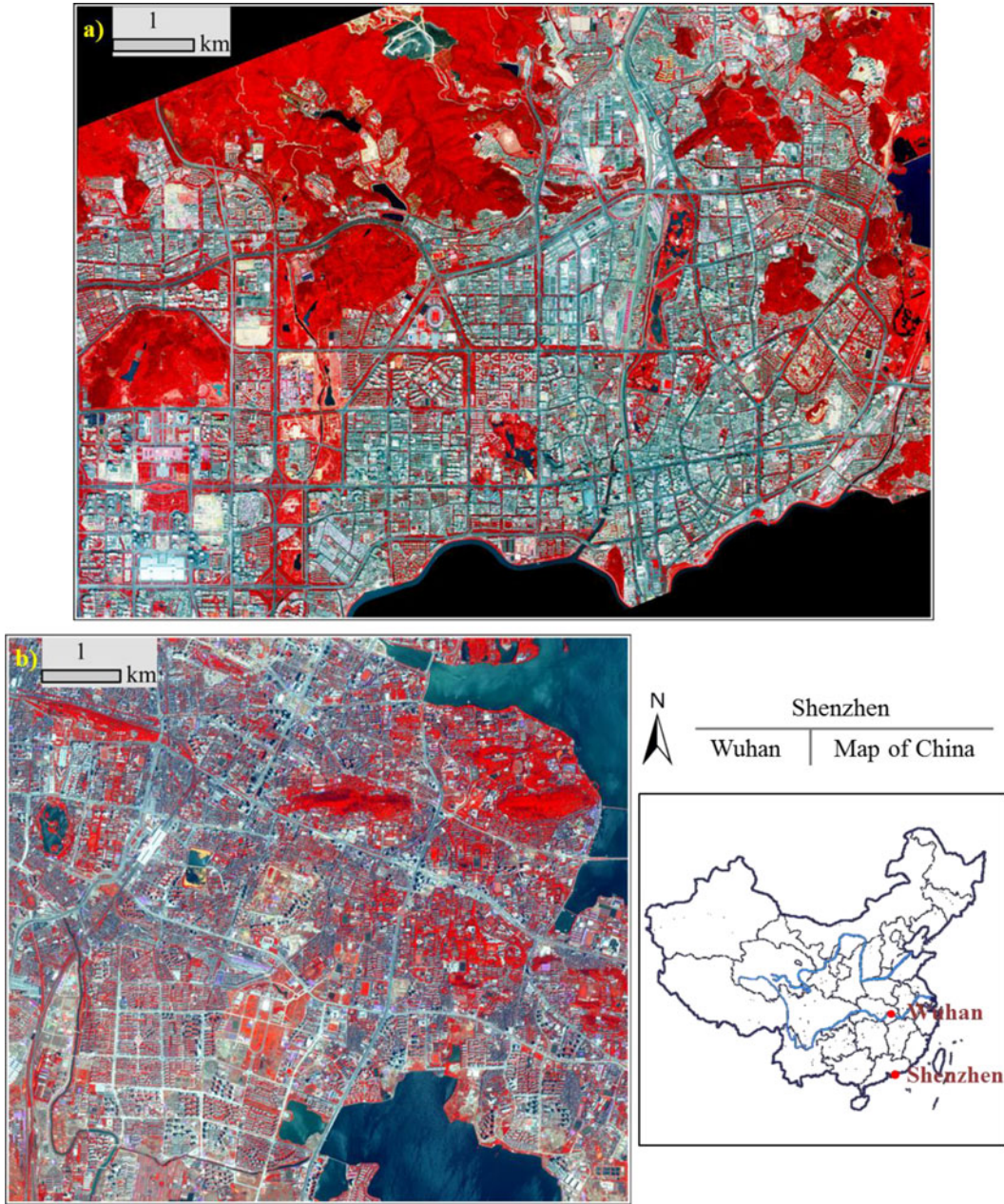


Fig. 1. Study areas of (a) Shenzhen and (b) Wuhan.

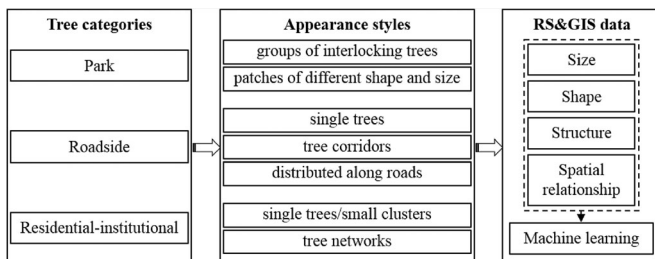


Fig. 2. Conceptual framework for the tree category identification.

### A. Pixel-Level Vegetation Extraction

Vegetation indices derived from the relevant spectral bands are widely used for the extraction of vegetation information.

The enhanced vegetation index (EVI) was designed to improve the sensitivity in high biomass regions and, at the same time, minimize soil and atmospheric influences through the inclusion of the blue (B) band [37]. The EVI is calculated using the reflective values of the near-infrared (NIR), red (R), and B bands [38]:

$$EVI = 2.5 \frac{NIR - R}{NIR + 6R - 7.5B + 1}. \quad (1)$$

Although the EVI is effective in recognizing vegetation, some cyan roofs can still be mistakenly identified as vegetation due to their similar spectral characteristic in the NIR (band 7), R (band 5), and B (band 2) bands (see Fig. 5). Based on this, we propose the verified EVI (VEVI) to remove the mixed cyan

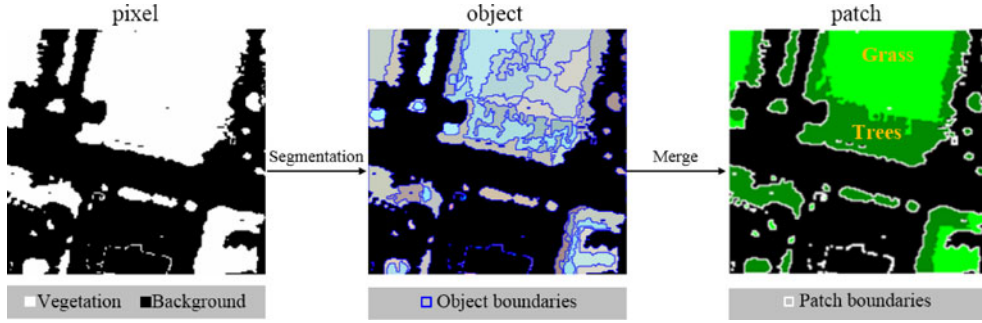


Fig. 3. Three processing units: pixel, object, and patch.

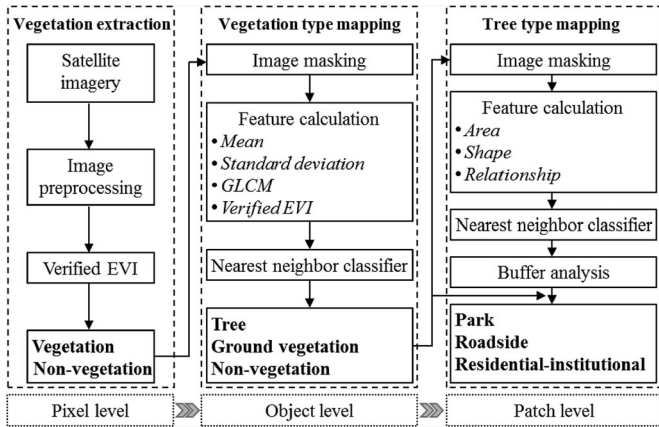


Fig. 4. Workflow for the proposed tree-type classification.

roofs by incorporating the spectral values in the green band ( $G$ ) as follows:

$$VEVI = 2.5 \frac{NIR - R}{NIR + 6R - 3.5B - 4G + 1}. \quad (2)$$

As shown in Fig. 5, the inclusion of the  $G$  band (band 3) in the VEVl can suppress the signal of cyan roofs and simultaneously enhance the vegetation signal, thereby performing better than the traditional EVI. This phenomenon can be attributed to the fact that the reflectance in the  $G$  (band 3) band is much greater than that in the other visible bands (band 5 and band 2) for cyan buildings. Ultimately, a vegetation map can be generated by simply setting a threshold for the index. A single threshold value is manually tuned based on visually examining the VEVl values for vegetation and nonvegetation pixels.

### B. Object-Level Vegetation-Type Mapping

Although the proposed pixel-level index is effective in extracting vegetation, it can still introduce some unavoidable errors due to the increase of the intraclass variance and the decrease of the interclass variance in the spectral domain of high spatial resolution images. Consequently, the vegetation map needs to be further refined, and the vegetation types (i.e., trees and ground vegetation) are classified in order to help the following tree-type classification. An object-based technique that analyzes

both the spectral and spatial information in each homogeneous segment is adopted, which has been demonstrated to be effective in the classification of high spatial resolution data [39], [40]. The proposed object-level process for vegetation-type classification (i.e., trees, ground vegetation, and nonvegetation) consists of three steps: 1) image segmentation; 2) object-specific feature calculation; and 3) classification (see Fig. 6). To acquire the vegetation objects, all eight bands masked with the pixel-level vegetation layer are used as the input for the multiresolution segmentation approach [41]. The size, shape, and compactness of the image objects are the key parameters in the segmentation. In our experiments, the image segmentation was conducted using a scale parameter of 100, a shape factor of 0.1, and a compactness factor of 0.5, which were manually determined by careful visual inspection. For each segment, the mean and standard deviation of each spectral band are calculated since they have the potential to discriminate between vegetation and nonvegetation. Additionally, the object-specific grey-level co-occurrence matrix (GLCM) [42] texture is calculated due to its effectiveness in capturing the textural difference between trees and ground vegetation objects [23]. The incorporation of both spectral and textural features means that the different features can complement each other in classifying trees, ground vegetation, and nonvegetation. Furthermore, the texture analysis of semantically meaningful objects rather than the traditional square kernels can avoid the selection of the window size, since image objects are potentially varied in size [39], [42]. Haralick [43] originally proposed 14 texture measures calculated from the GLCM, the selection of which should be case- and class-specific [44]. Specifically, in our study, homogeneity and entropy, which measure contrast and orderliness, respectively, are employed according to the suggestions made in [39] and [45]. The directionally invariant texture measures are calculated by taking the average value of the texture results over all four directions ( $0^\circ$ ,  $45^\circ$ ,  $90^\circ$ , and  $135^\circ$ ). The calculation of the object-based features is followed by classification of the image objects. The nearest neighbor classifier based on the Euclidean distance is used in this study because: 1) it is a nonparametric classifier, as no assumption of the data distribution is required; and 2) it has good generality and transferability capabilities [46], [47]. In the object-level classification, the simple 1-nearest neighbor (1NN) classifier is employed since the error rate for 1NN is never larger than twice the optimal error rate [48]. Based on the

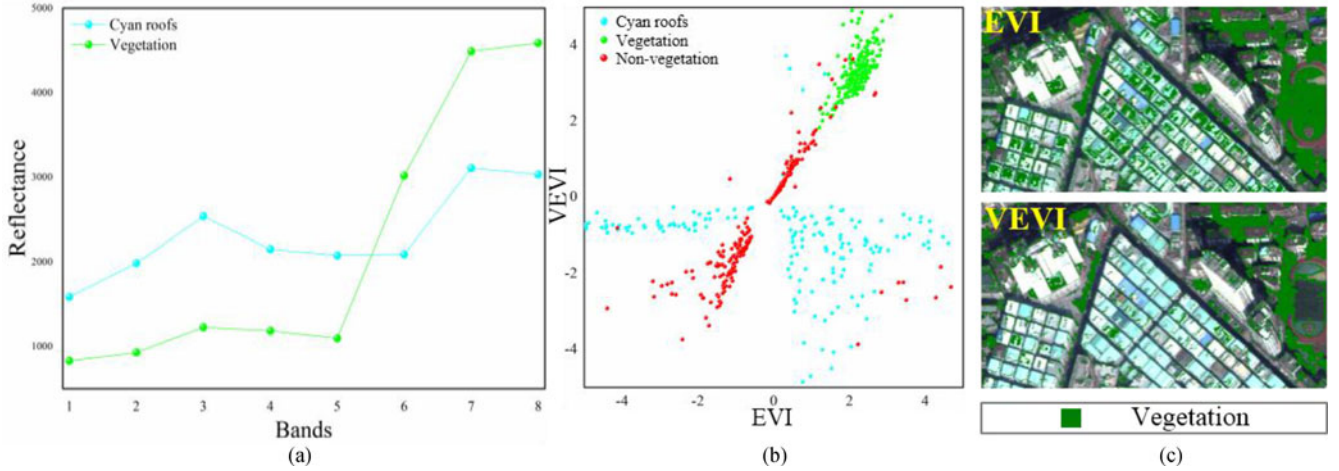


Fig. 5. Comparison between the EVI and the VEV in high-resolution imagery: (a) spectral curves of cyan roofs and vegetation; (b) scatter plots for cyan roofs, vegetation, and nonvegetation in the VEV-EVI space; and (c) example of vegetation extraction using the two vegetation indices.

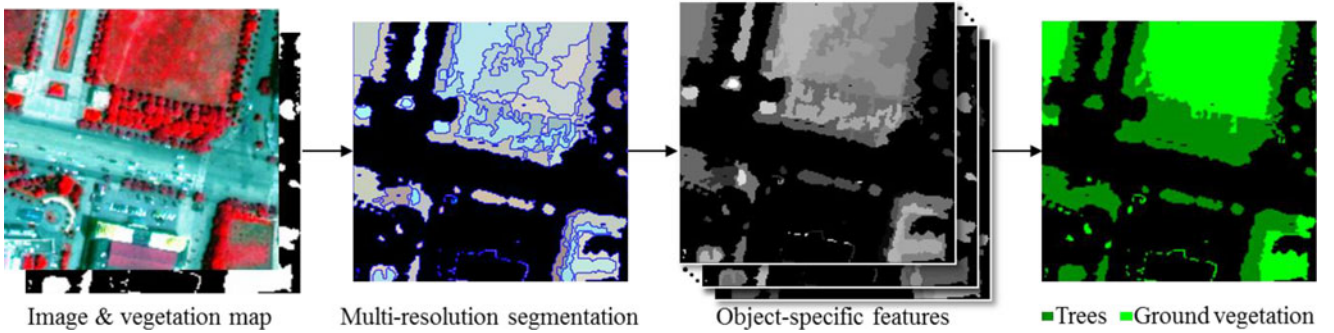


Fig. 6. Framework for the object-level vegetation-type mapping.

extracted features (i.e., the mean and standard deviation of the spectral bands, the textural measures, and the VEV) and the 1NN classifier, the refined vegetation map, as well as the vegetation types (i.e., tree and ground vegetation), can be obtained as the final product at the object level (see Fig. 4).

### C. Patch-Level Tree-Type Mapping

As stated earlier, the semantic categories of trees (i.e., park, roadside, and residential–institutional trees) from an urban habitat perspective can be identified by considering the size, shape, structure, and spatial relationship. Based on this, tree-type mapping at the patch level is proposed with the following steps.

1) *Vegetation Patch Derivation*: The accurate vegetation map derived at the object level is used to generate vegetation patches. As shown in Fig. 3, “vegetation patch” refers to the image regions formed by the spatially connected vegetation objects, and they serve as the basic unit to describe the three categories, based on the fact that they are aggregated as patches with different spatial patterns. For vegetation patch derivation, the adjacent vegetation objects are spatially merged into a patch. This process is repeated until no adjacent vegetation objects can be merged.

2) *Patch-Level Metrics Calculation*: A series of patch-level metrics that can quantitatively describe the spatial patterns are

calculated [49], [50]. The patch-level metrics considered in our study include the size and shape of the patch, which are calculated using FRAGSTATS [51], and the distance to the nearest major road, depicting the spatial relationship between the vegetation patch and road. Details of the patch-level metrics can be found in Table I. It should be noted that the map of major roads was derived from OSM due to its advantage of free availability [52].

3) *Patch-Level Classification*: To examine the discriminative ability among the three urban habitat types with each selected patch-level metric, box plots indicating feature distribution versus categories are shown in Fig. 7. A satisfactory discrimination between park and roadside/residential–institutional vegetation is observed using the patch-level metrics. In addition, there is considerable overlap between roadside and residential–institutional vegetation in the boxes of the area and shape attributes. Meanwhile, a better separability between roadside and residential–institutional vegetation can be acquired using the DR attribute. In this regard, a two-stage classification framework is proposed to classify the park, roadside, and residential–institutional vegetation. In the first stage, the patch-level metrics are input into the nearest neighbor classifier to identify park and roadside/residential–institutional vegetation. Here, the number of nearest neighbors is optimized based on the leave-one-out error on training samples. In the

TABLE I  
OVERVIEW OF THE METRICS CONSIDERED IN THIS STUDY

Level	Metric	Description
Patch	Area (AREA)	The area of each patch comprising a landscape mosaic.
	Perimeter-area ratio (PARA)	The ratio of the patch perimeter to area, reflecting the shape complexity.
	Shape index (SHAPE)	Patch perimeter divided by the minimum perimeter possible for a maximally compact patch of the corresponding patch area.
	Fractal dimension index (FDI)	Calculated by regressing the log of the patch perimeter against the log of the patch area.
	Related circumscribing circle (RCC)	The patch area divided by the area of the smallest circle that can circumscribe the patch.
	Contiguity index (CI)	A measure of the spatial connectedness, calculated as the proportion of connected cells within a patch.
	Euclidean nearest neighbor distance (ENND)	Distance of each patch to the nearest neighbor patch.
Class	Distance to road (DR)	Distance of each patch to the road.
	Percentage of landscape (PLAND)	Percentage of the landscape occupied by the corresponding class.
	Patch density (PD)	Number of patches per square meter for the corresponding class.
	Perimeter-area fractal dimension (PAFR)	A measure of shape complexity for the corresponding class.
	Cohesion index (CI)	A measure of the physical connectedness of the corresponding class.
Landscape	Aggregation index (AI)	Computed as the ratio between the number of like adjacencies and the maximum possible number of like adjacencies.
	Shannon's diversity index (SHDI)	A measure of the diversity of the land cover in a landscape.

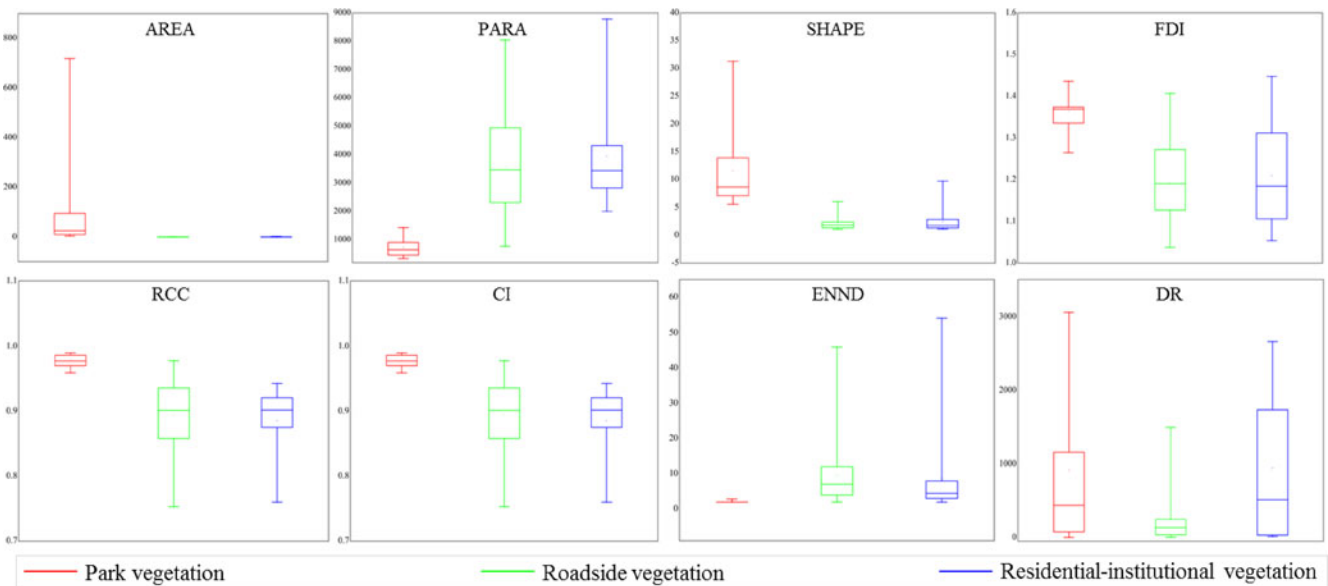


Fig. 7. Box plots showing the feature distribution of park, roadside, and residential-institutional vegetation at the patch level. The central box indicates the 25th percentile (closest to zero), the median, and the 75th percentile, and the whiskers show the range of the data.

second stage, a buffer analysis is used to identify roadside and residential-institutional vegetation on the basis of the spatial relationship with road. The road buffer zones are constructed with a buffer size of 25 m, in accordance with the average width of the boundary line of roads from the “Code for Transport Planning on Urban Road” [53]. The two vegetation types can be simply categorized based on whether the vegetation objects fall inside or outside the buffer zone. Subsequently, the result of the urban habitat is masked by the map of trees derived at the object level. In this way, the final product, i.e., the semantic categories of the urban trees, can be generated. Note that, in an urban environment, ground vegetation can serve the same ecological and landscape function as trees, but may also constitute cultivated land, aquatic plants, and so on, which is more complicated for type classification from an urban habitat perspective.

#### D. Class- and Landscape-Level Analysis

Based on the map of park, roadside, and residential-institutional trees, we attempt here to conduct a quantitative analysis of their composition and configuration at the class and landscape levels, which is important for urban ecological environment management and planning. Manual correction of the classification results is needed to ensure the fidelity of the analysis. In order to conduct a comprehensive landscape analysis, a series of class- and landscape-level metrics are considered:

- 1) percentage of landscape (PLAND);
- 2) patch density (PD);
- 3) perimeter-area fractal dimension (PAFRAC);
- 4) cohesion index (CI);
- 5) aggregation index (AI); and
- 6) Shannon's diversity index (SHDI) [54].

TABLE II  
ERROR MATRIX AND ACCURACY ASSESSMENT FOR THE TREE-TYPE  
CLASSIFICATION

Accuracy assessment for Shenzhen					
Classified data	Reference data			Total	User's acc.
	Park	Residential–institutional	Roadside		
Park	8	1	0	9	88.9%
Residential–institutional	4	47	7	58	81.0%
Roadside	0	1	42	43	97.7%
Background	0	1	2		
#Number of samples	12	50	51		
Producer's acc.	66.7%	94.0%	82.4%		<b>Overall: 85.8%</b>
Accuracy assessment for Wuhan					
Classified data	Reference data			Total	User's acc.
	Park	Residential–institutional	Roadside		
Park	2	0	0	2	100.0%
Residential–institutional	2	19	2	23	82.6%
Roadside	0	1	23	24	95.8%
Background	0	0	2		
#Number of samples	4	20	27		
Producer's acc.	50.0%	95.0%	85.2%		<b>Overall: 86.3%</b>

These metrics can reflect the landscape characteristic from the aspects of composition, fragmentation, shape complexity, connectedness, aggregation, and diversity [55], [56]. Details of the above-mentioned metrics can be found in Table I.

#### IV. RESULTS

In order to evaluate the effectiveness of the proposed methodology, the results were validated using a confusion matrix for the quantitative evaluation and visual inspection for the quality of the patch boundaries.

##### A. Accuracy Assessment

For the quantitative evaluation, samples were collected for the whole study area. The samples were manually interpreted using the satellite imagery with the help of ancillary information from the field or online maps. Note that the basic unit for our collected samples is a patch rather than a pixel. In the Shenzhen (Wuhan) study area, the sample sizes for park, residential–institutional, and roadside trees were 23 (7), 100 (40), and 100 (52), respectively. To allow an accurate estimation of the classification accuracies, confusion matrices (see Table II) based on two-fold cross validation with five random splits were generated. As shown in Table II, overall, the proposed tree-type classification method can achieve a satisfactory performance. The overall classification accuracy is 85.8% and 86.3% for the Shenzhen and Wuhan study areas, respectively. In addition, from the confusion matrices (see Table II), we can conclude that all the tree types are classified with acceptable accuracies. For the park identification, 8 patches out of 12 reference patches are correctly detected in Shenzhen (66.7%) and 2 park patches out of 4 patches are detected in Wuhan (50.0%). For the Shenzhen data, 47 out of 50 residential–institutional tree patches are correctly

TABLE III  
COMPUTATION TIMES FOR THE PROPOSED METHOD (IN SECONDS)

Image subset	Pixel	Object	Patch	Total
A	0.1	24.3	27.6	52
B	0.1	18.9	29.7	48.7
C	0.1	23.2	29.4	52.7

identified (94.0%), with 1 patch for each of the misclassified categories (i.e., park, roadside, and background). Likewise, for Wuhan, the proposed method correctly identifies 19 roadside tree patches out of 20 reference patches (95.0%). For the roadside tree identification, a total of 42 patches for Shenzhen are identified among 51 reference patches (82.4%). The proposed method can detect 23 out of 27 patches, indicating a producer's accuracy of 85.2%. The user's accuracies for all the categories are larger than 80.0%. Furthermore, a part of a patch can be mistakenly classified due to the fact that roadside/residential–institutional trees are sometimes spatially connected to park. This error is introduced at the vegetation patch derivation step.

##### B. Visual Inspection

For the visual inspection, three image subsets [(A), (B), and (C)] were chosen from the study areas. The corresponding semantic classification results of urban trees overlaid with the reference objects are presented in order to evaluate the quality of the identified patch boundaries (as shown in Fig. 8). The three image subsets represent contexts that are challenging for mapping, with widely differing canopy sizes, different tree types, and varying spatial patterns. As can be seen from Fig. 8, overall, a good agreement between the detected tree crowns and reference object boundaries can be observed, with only a few under- and over-identification errors. The over-identification can be attributed to over-segmentation in the transition areas between tree crown and ground vegetation. Some of the tree crowns are not detected due to their small size or the insignificant contrast in spectral and textural measures with respect to ground vegetation. As shown in Fig. 8(B), there is some confusion between the roadside and residential–institutional trees, due to their spatial connection. In Fig. 8(C), the trees in the residential area next to the park are wrongly identified as park trees.

##### C. Computation Time

Since the computation time is also an important factor of an algorithm, the computation time of the proposed method is presented in Table III. The computation times are evaluated for the three image subsets in Fig. 8, and the computation times at the pixel, object, and patch level are also presented. The pixel-level vegetation extraction and patch-level classification were implemented in MATLAB 2012a. The object-level vegetation classification was conducted via eCognition Developer. The personal computer used had a 3.07 GHz Intel Core i3 CPU and 16 GB of RAM. In general, the proposed method has a satisfactory computational efficiency, with computation times of less than 1 min for the three image subsets. The computation time is related to the image size, and the numbers of objects and patches to be

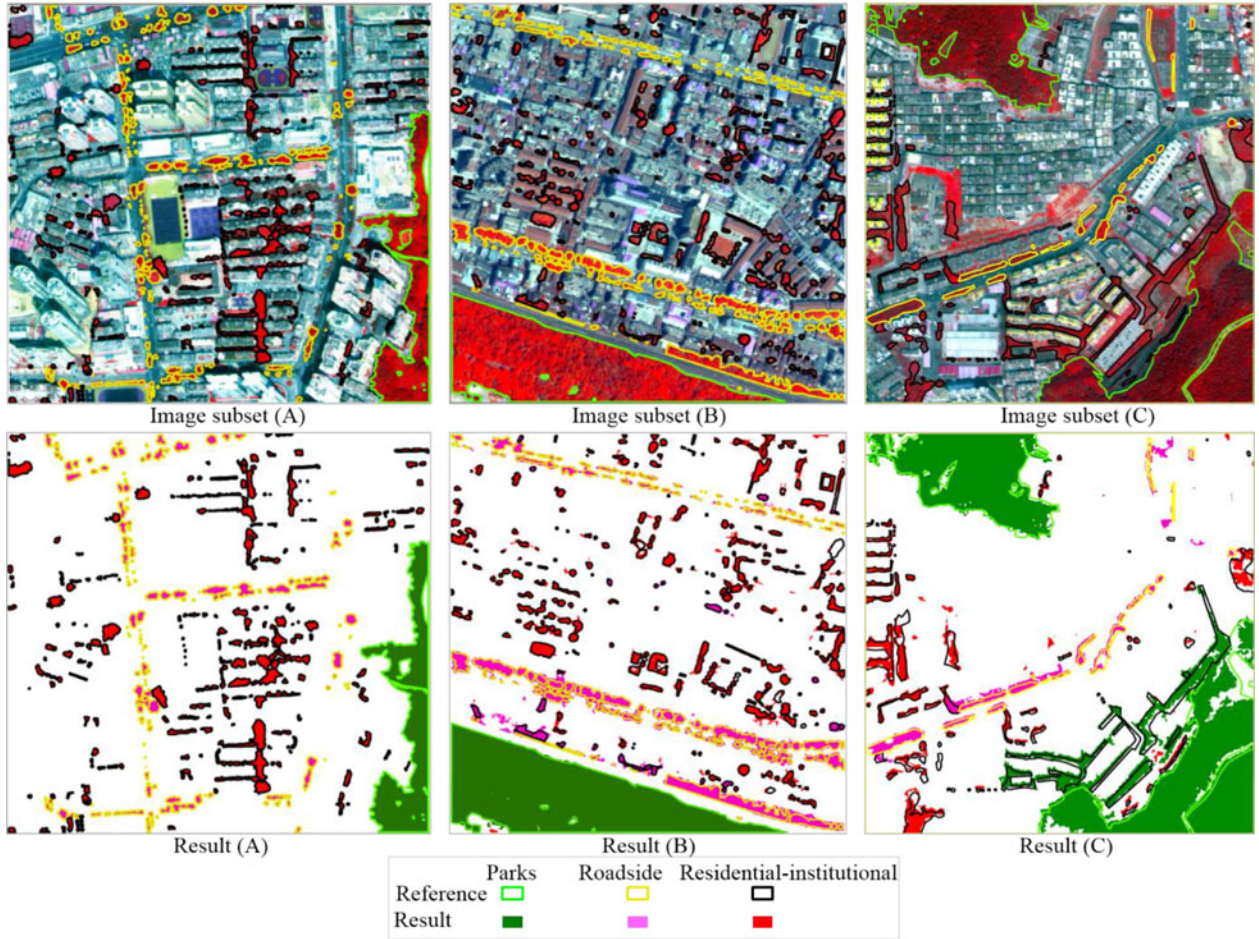


Fig. 8. Instances of the tree-type identification results.

processed. It is worth noting that the computational efficiency could be further optimized by the use of C programming or advanced computing devices such as a graphics processing unit.

## V. DISCUSSION

### A. Comparison With an Object-Based Method

Since no other studies related to the semantic classification of urban trees were found, a method used for identifying tree species was employed for the comparison. The object-based method proposed by Pu *et al.* [27] that uses eight WorldView-2 bands plus five normalized difference vegetation indices was used, which was originally designed for identifying tree species, and not habitats. For a fair comparison, the training samples and validation samples developed at the patch level were used, and the accuracy was evaluated at the patch level by majority voting. The  $F$ -measure (the harmonic mean of the user's and producer's accuracy) for each class and the overall accuracy (OA) of the proposed and compared methods are presented in Table IV. In general, the proposed method outperforms the compared method. It should, however, be noted that the great difference in the accuracies of the proposed method and the method of Pu *et al.* [27] is caused by the inconsistent research objectives. The spectral bands and spectral indices can be useful to distinguish roadside trees, but the residential-institutional trees are

TABLE IV  
ACCURACIES FOR THE PROPOSED AND COMPARED METHODS

Methods	Park	Res.-Int.	Roadside	OA
Proposed	76.2	87.0	89.4	85.8
[27]	55.6	0	90.7	64.1

mistakenly identified as park trees due to their similar spectral characteristics. The limited ability of the spectral features at the object level to discriminate the three categories can be attributed to the complex composition of the different tree species in the park, roadside, and residential-institutional categories.

### B. Effectiveness of the Proposed Method

The existing studies of urban tree mapping have mainly concentrated on tree extraction [5], [22], [23] or tree species identification [4], [9], [14], [25], [57]–[59], and they have neglected the semantic categorization of urban trees. As such, in this study, we have proposed a novel method for the semantic classification of urban trees. The differences between the existing studies and the proposed method are detailed below.

First, the semantic attributes, i.e., park, roadside, and residential-institutional trees, are further classified based upon tree extraction. There have been a large number of studies

devoted to tree extraction [5], [22], [23]. Among these studies, the recent study by Ardila *et al.* [23] formulated a series of methods that were designed for specific urban contexts (e.g., individual trees, groups of trees, and trees along roads). The context-sensitive extraction of tree crown objects can effectively outline tree crowns, but no attributes (i.e., semantic categories) of the trees can be generated. In addition, the study by Zhao *et al.* [60] focused on roadside tree extraction in a small study area. In short, to date, no previous studies have addressed the categorization of urban trees according to their semantic attributes, i.e., categories cognized and conceptualized by humans, such as park, roadside, and residential–institutional trees, which serve as different urban ecological functions.

Second, there are significant differences between the semantic classification of urban trees (i.e., park, roadside, and residential–institutional) considered in this study and the tree species classification (e.g., palm and privet) considered in the existing studies. The tree categories in our study are defined from an urban habitat perspective. However, the systems for the categorization of tree species are different in tropical forest [4], mixed forest [58], rain forest [59], and urban forest [9], [14], [25]. Furthermore, even for tree species mapping in urban forests, the categories can be diverse due to the different climate conditions, as well as the urban planning and management regimes in different cities [9], [14], [25]. However, the tree types from an urban habitat perspective can provide unified semantic categories for urban tree mapping.

Third, different features and processing units are considered. The three-level (i.e., pixel, object, and patch) system is considered in order to capture features for urban habitat discrimination in an effective and efficient way. At the pixel level, the vegetation mask is generated to avoid the heavy computational burden of the nonvegetated areas, which is essential, especially for large-area vegetation mapping. At the object level, the masked vegetated areas are separated into trees and ground vegetation using object-specific features (i.e., the spectral and textual features), which is based on the previous research [39], [42] into vegetation-type mapping. The object-level processing is aimed at delineating the tree crowns and removing the false alarms in the pixel-level vegetation extraction. Subsequently, at the patch level, the size, shape, structure, and spatial relationship are considered for the identification of the three urban habitat types. As a result, the urban habitats aggregated in different spatial patterns are mapped using remote sensing data, filling a large gap in the existing studies.

Finally, two typical megacities, Shenzhen and Wuhan, with coverage areas of 79.35 and 56.75 km<sup>2</sup>, respectively, were tested in this study, which is sufficient to illustrate the robustness and effectiveness of the proposed approach. Moreover, both quantitative and qualitative accuracy evaluations were undertaken, and indicated a satisfactory performance.

### C. Composition and Configuration of the Three Tree Categories

Quantitative measures were calculated in order to reveal the characteristics of the landscape composition and the configu-

TABLE V  
QUANTITATIVE MEASURES OF THE TREE COMPOSITION AND CONFIGURATION AT THE CLASS AND LANDSCAPE LEVELS

	Shenzhen			Wuhan		
	Park	Roadside	Res.–Int.	Park	Roadside	Res.–Int.
PLAND	21.42	2.87	6.66	4.42	2.34	17.07
PD	1.29	43.73	196.33	0.33	71.44	296.97
PAFR	1.42	1.44	1.27	1.39	1.45	1.45
CI	99.95	97.64	98.16	99.90	97.57	99.23
AI	98.59	92.34	92.28	98.07	90.56	92.51
SHDI		0.81			0.78	

ration of the three tree categories (see Table V). The results indicate some interesting points:

- 1) park trees take up 21.42% of the Shenzhen study area, constituting the dominant natural landscape component, and, in Wuhan, residential–institutional trees make up the largest proportion (17.07%) of the three urban habitat types;
- 2) there is a more significant discrepancy for PLAND between roadside trees (2.34%) and residential–institutional trees (17.07%) in Wuhan than in Shenzhen (the PLAND for roadside and residential–institutional trees is 2.87% and 6.66%, respectively);
- 3) the residential–institutional trees show the largest PD value, followed by roadside and park, indicating greater fragmentation and spatial heterogeneity;
- 4) the PAFRAC yields no clear patterns across over the three types, but the residential–institutional trees in Shenzhen (1.27) and the park trees in Wuhan (1.39) have the lowest dimensions, representing a simpler shape complexity;
- 5) park trees have the largest values in both the cohesion and aggregation indices, suggesting the maximum physical connectedness and aggregation; and
- 6) the SHDI is 0.81 and 0.78 for Shenzhen and Wuhan, respectively, demonstrating that the natural landscape in Shenzhen is more diverse.

In conclusion, the composition and configuration metrics in the two cities show some general characteristics, such as greater fragmentation and spatial heterogeneity for residential–institutional trees and maximum physical connectedness and aggregation for park trees.

### D. Limitations of the Proposed Method

There are some limitations to the proposed method. First, the road network information provided by OSM can help to discriminate between roadside and residential–institutional trees. Unfortunately, the OSM road networks are not always available or complete, which may affect the applicability of the proposed method in other urban areas. However, it should be noted that volunteered geographic information is the cheapest and sometimes the only source of GIS data, especially in areas where access to geographic information is constrained due to national security [61]. Second, the urban habitats are mapped based on the assumption that they are spatially aggregated patches with

varied spatial patterns; however, there may be some spatial connectedness between the three urban habitat types. In this situation, identification mistakes can be introduced in the patch derivation process, which require manual correction before the further analysis. Conditional aggregation using certain metrics will, therefore, be considered in our further research. Third, the segmentation quality can affect the mapping accuracy to a certain extent, due to the large within-crown spectral variation. In addition, the segmentation parameters are sensor- and scene-specific, indicating that they should be modified when different data or study areas are used, in order to achieve a segmentation quality that is as high as possible. Finally, the use of a supervised method requires the construction of a sample set that is representative of the study area, which is a common problem for the supervised approaches.

## VI. CONCLUSION

In this study, a novel pixel-object-patch three-level framework has been proposed for the semantic classification of urban trees from an urban habitat perspective using VHR remote sensing imagery. The results derived from both the Shenzhen and Wuhan WorldView-2 data sets confirm the potential and effectiveness of the proposed method. The notable advantages of the proposed method are as follows:

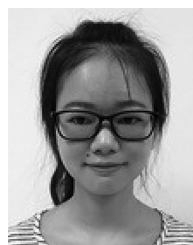
- 1) The vegetation extraction at the pixel level is the key step for reducing the computational cost in the further steps, since the information index (VEVI) can be used to easily mask out other urban structures.
- 2) In line with previous research, object-specific spectral and textural features are employed for the vegetation mapping. At the object level, the nonvegetation information is further filtered out, and discrimination between trees and ground vegetation is achieved.
- 3) A series of patch-level metrics that depict the area, shape, structure, and spatial relationship are considered for the urban habitat type classification. The experimental results indicate that these metrics are effective as they can capture the intrinsic characteristics of the different appearance styles.
- 4) Through the landscape composition and configuration of the three tree categories, greater fragmentation and spatial heterogeneity for residential-institutional trees is observed, and park trees tend to show the maximum physical connectedness and aggregation.

The proposed framework allows the user to map park, roadside, and residential-institutional trees in a generalized way, which could help to inform policies related to urban ecosystems. However, considerable additional work is needed to test the robustness and applicability of the proposed method in other urban areas with different ecological structures. It will also be necessary to find more effective features or classifiers for the semantic classification of urban trees. In addition, the three urban habitat types may have varying degrees of urban heat island mitigation, and they could be related to socioeconomic factors (e.g., real estate prices), which needs to be analyzed quantitatively in our future work.

## REFERENCES

- [1] P. Bolund and S. Hunhammar, "Ecosystem services in urban areas," *Ecol. Econ.*, vol. 29, no. 2, pp. 293–301, 1999.
- [2] T. Hartig and P. H. Kahn, "Living in cities, naturally," *Science*, vol. 352, no. 6288, pp. 938–940, 2016.
- [3] F. E. Kuo and W. C. Sullivan, "Environment and crime in the inner city does vegetation reduce crime?" *Environ. Behav.*, vol. 33, no. 3, pp. 343–367, 2001.
- [4] W. S. Walker, C. M. Stickler, J. M. Kellendorfer, K. M. Kirsch, and D. C. Nepstad, "Large-area classification and mapping of forest and land cover in the Brazilian Amazon: A comparative analysis of ALOS/PALSAR and Landsat data sources," *IEEE J. Sel. Topics Appl. Earth Observ. Remote Sens.*, vol. 3, no. 4, pp. 594–604, Dec. 2010.
- [5] J. P. Ardila, W. Bijker, V. A. Tolpekin, and A. Stein, "Quantification of crown changes and change uncertainty of trees in an urban environment," *ISPRS J. Photogramm. Remote Sens.*, vol. 74, pp. 41–55, 2012.
- [6] K. T. Ward and G. R. Johnson, "Geospatial methods provide timely and comprehensive urban forest information," *Urban Forestry Urban Greening*, vol. 6, no. 1, pp. 15–22, 2007.
- [7] C. Freeman and O. Buck, "Development of an ecological mapping methodology for urban areas in New Zealand," *Landscape Urban Plan.*, vol. 63, no. 3, pp. 161–173, 2003.
- [8] C. Iovan, D. Boldo, and M. Cord, "Detection, characterization, and modeling vegetation in urban areas from high-resolution aerial imagery," *IEEE J. Sel. Topics Appl. Earth Observ. Remote Sens.*, vol. 1, no. 3, pp. 206–213, Sep. 2008.
- [9] M. Alonzo, B. Bookhagen, and D. A. Roberts, "Urban tree species mapping using hyperspectral and lidar data fusion," *Remote Sens. Environ.*, vol. 148, pp. 70–83, 2014.
- [10] J. Nichol and C. Lee, "Urban vegetation monitoring in Hong Kong using high resolution multispectral images," *Int. J. Remote Sens.*, vol. 26, no. 5, pp. 903–918, 2005.
- [11] R. D. Graetz, "Remote sensing of terrestrial ecosystem structure: An ecologist's pragmatic view," *Remote Sens. Biosphere Funct.*, vol. 79, pp. 5–30, 1990.
- [12] S. J. Walsh, "Coniferous tree species mapping using Landsat data," *Remote Sens. Environ.*, vol. 9, pp. 11–26, 1980.
- [13] E. C. B. de Colstoun, M. H. Story, C. Thompson, K. Commisso, T. G. Smith, and J. R. Irons, "National park vegetation mapping using multitemporal Landsat 7 data and a decision tree classifier," *Remote Sens. Environ.*, vol. 85, pp. 316–327, 2003.
- [14] R. Pu and S. Landry, "A comparative analysis of high spatial resolution IKONOS and WorldView-2 imagery for mapping urban tree species," *Remote Sens. Environ.*, vol. 124, pp. 516–533, 2012.
- [15] P. Potapov, S. Turubanova, and M. C. Hansen, "Regional-scale boreal forest cover and change mapping using Landsat data composites for European Russia," *Remote Sens. Environ.*, vol. 115, pp. 548–561, 2011.
- [16] M. Schwarz and N. E. Zimmermann, "A new GLM-based method for mapping tree cover continuous fields using regional MODIS reflectance data," *Remote Sens. Environ.*, vol. 95, pp. 428–443, 2005.
- [17] Y. Shao and R. S. Lunetta, "Sub-pixel mapping of tree canopy, impervious surfaces, and cropland in the Laurentian Great Lakes Basin using MODIS time-series data," *IEEE J. Sel. Topics Appl. Earth Observ. Remote Sens.*, vol. 4, no. 2, pp. 336–347, Jun. 2011.
- [18] M. Hansen, R. DeFries, J. Townshend, M. Carroll, C. Dimiceli, and R. Sohlberg, "Global percent tree cover at a spatial resolution of 500 meters: First results of the MODIS vegetation continuous fields algorithm," *Earth Interact.*, vol. 7, no. 10, pp. 1–15, 2003.
- [19] M. C. Hansen *et al.*, "High-resolution global maps of 21st-century forest cover change," *Science*, vol. 342, no. 6160, pp. 850–853, 2013.
- [20] X. Huang and L. Zhang, "An SVM ensemble approach combining spectral, structural, and semantic features for the classification of high-resolution remotely sensed imagery," *IEEE Trans. Geosci. Remote Sens.*, vol. 51, no. 1, pp. 257–272, Jan. 2013.
- [21] X. Huang, Q. Lu, and L. Zhang, "A multi-index learning approach for classification of high-resolution remotely sensed images over urban areas," *ISPRS J. Photogramm. Remote Sens.*, vol. 90, pp. 36–48, 2014.
- [22] J. P. Ardila, V. A. Tolpekin, W. Bijker, and A. Stein, "Markov-random-field-based super-resolution mapping for identification of urban trees in VHR images," *ISPRS J. Photogramm. Remote Sens.*, vol. 66, pp. 762–775, 2011.
- [23] J. P. Ardila, W. Bijker, V. A. Tolpekin, and A. Stein, "Context-sensitive extraction of tree crown objects in urban areas using VHR satellite images," *Int. J. Appl. Earth Observ. Geoinf.*, vol. 15, pp. 57–69, 2012.

- [24] M. Dalponte, H. O. Ørka, L. T. Ene, T. Gobakken, and E. Næsset, "Tree crown delineation and tree species classification in boreal forests using hyperspectral and ALS data," *Remote Sens. Environ.*, vol. 140, pp. 306–317, 2014.
- [25] J. Zhou, J. Qin, and S. Xu, "Feature-location analyses for identification of urban tree species from very high resolution remote sensing data," *Ecol. Informat.*, vol. 29, pp. 16–24, 2015.
- [26] J. Lee *et al.*, "Individual tree species classification from airborne multi-sensor imagery using robust PCA," *IEEE J. Sel. Topics Appl. Earth Observ. Remote Sens.*, vol. 9, no. 6, pp. 2554–2567, Jun. 2016.
- [27] R. Pu, S. Landry, and J. Zhang, "Evaluation of atmospheric correction methods in identifying urban tree species with WorldView-2 imagery," *IEEE J. Sel. Topics Appl. Earth Observ. Remote Sens.*, vol. 8, no. 5, pp. 1886–1897, May 2015.
- [28] C. Jim, "Outstanding remnants of nature in compact cities: Patterns and preservation of heritage trees in Guangzhou city (China)," *Geoforum*, vol. 36, no. 3, pp. 371–385, 2005.
- [29] F. Li, R. Wang, J. Paulussen, and X. Liu, "Comprehensive concept planning of urban greening based on ecological principles: A case study in Beijing, China," *Landscape Urban Plan.*, vol. 72, no. 4, pp. 325–336, 2005.
- [30] A. B. Cumming, M. F. Galvin, R. J. Rabaglia, J. R. Cumming, and D. B. Twardus, "Forest health monitoring protocol applied to roadside trees in Maryland," *J. Arboriculture*, vol. 27, no. 3, pp. 126–138, 2001.
- [31] M. Seymour, J. Wolch, K. D. Reynolds, and H. Bradbury, "Resident perceptions of urban alleys and alley greening," *Appl. Geography*, vol. 30, no. 3, pp. 380–393, 2010.
- [32] C. Jim and H. Liu, "Patterns and dynamics of urban forests in relation to land use and development history in Guangzhou City, China," *Geographical J.*, vol. 167, no. 4, pp. 358–375, 2001.
- [33] C. Jim and H. Liu, "Species diversity of three major urban forest types in Guangzhou City, China," *Forest Ecol. Manage.*, vol. 146, no. 1, pp. 99–114, 2001.
- [34] C. Jim, "Land use and amenity trees in urban Hong Kong," *Land Use Policy*, vol. 4, no. 4, pp. 281–293, 1987.
- [35] C. Gong, J. Chen, and S. Yu, "Biotic homogenization and differentiation of the flora in artificial and near-natural habitats across urban green spaces," *Landscape Urban Plan.*, vol. 120, pp. 158–169, 2013.
- [36] L. Wang, W. Gong, Y. Ma, and M. Zhang, "Modeling regional vegetation NPP variations and their relationships with climatic parameters in Wuhan, China," *Earth Interact.*, vol. 17, no. 4, pp. 1–20, 2013.
- [37] Z. Jiang, A. R. Huete, K. Didan, and T. Miura, "Development of a two-band enhanced vegetation index without a blue band," *Remote Sens. Environ.*, vol. 112, pp. 3833–3845, Oct. 2008.
- [38] A. Huete, H. Liu, K. V. Batchily, and W. Van Leeuwen, "A comparison of vegetation indices over a global set of TM images for EOS-MODIS," *Remote Sens. Environ.*, vol. 59, pp. 440–451, 1997.
- [39] C. Zhang and Z. Xie, "Combining object-based texture measures with a neural network for vegetation mapping in the Everglades from hyperspectral imagery," *Remote Sens. Environ.*, vol. 124, pp. 310–320, 2012.
- [40] R. Mathieu and J. Aryal, "Object-based classification of Ikonos imagery for mapping large-scale vegetation communities in urban areas," *Sensors*, vol. 7, no. 11, pp. 2860–2880, 2007.
- [41] M. Baatz and A. Schäpe, "Multiresolution segmentation: An optimization approach for high quality multi-scale image segmentation," in *Proc. Angewandte Geographische Informationsverarbeitung XII. Beiträ zum AGIT-Symp. Salzburg 2000*, Karlsruhe, Germany, 2000, pp. 12–23.
- [42] M. Kim, M. Madden, and T. A. Warner, "Forest type mapping using object-specific texture measures from multispectral ikonos imagery," *Photogramm. Eng. Remote Sens.*, vol. 75, no. 7, pp. 819–829, 2009.
- [43] R. M. Haralick, "Statistical and structural approaches to texture," *Proc. IEEE*, vol. 67, no. 5, pp. 786–804, May 1979.
- [44] T. Warner, "Kernel-based texture in remote sensing image classification," *Geography Compass*, vol. 5, no. 10, pp. 781–798, 2011.
- [45] P. D. Culbert, A. M. Pidgeon, V. S. Louis, D. Bash, and V. C. Radeloff, "The impact of phenological variation on texture measures of remotely sensed imagery," *IEEE J. Sel. Topics Appl. Earth Observ. Remote Sens.*, vol. 2, no. 4, pp. 299–309, Dec. 2009.
- [46] E. Ivits and B. Koch, "Object-oriented remote sensing tools for biodiversity assessment: A European approach," in *Proc. 22nd Eur. Assoc. Remote Sens. Lab. Symp.*, 2002, pp. 04–06.
- [47] S. W. Myint, P. Gober, A. Brazel, S. Grossman-Clarke, and Q. Weng, "Per-pixel versus. object-based classification of urban land cover extraction using high spatial resolution imagery," *Remote Sens. Environ.*, vol. 115, pp. 1145–1161, 2011.
- [48] B. S. Harish, D. S. Guru, and S. Manjunath, "Representation and classification of text documents: A brief review," *Int. J. Comput. Appl.*, vol. 8, no. 2, pp. 110–119, 2010.
- [49] H. Olf and M. E. Ritchie, "Fragmented nature: Consequences for biodiversity," *Landscape Urban Plan.*, vol. 58, no. 2, pp. 83–92, 2002.
- [50] G. Chust, D. Ducrot, and J. L. Pretus, "Land cover mapping with patch-derived landscape indices," *Landscape Urban Plan.*, vol. 69, no. 4, x pp. 437–449, 2004.
- [51] K. McGarigal and B. J. Marks, "FRAGSTATS: Spatial pattern analysis program for quantifying landscape structure," Oregon State Univ., Corvallis, OR, USA, Tech. Rep. 2.0, 1995.
- [52] Z. Guo, S. Du, and A. Habib, "An extended random walker approach for object extraction by integrating VGI data and VHR image," *IEEE J. Sel. Topics Appl. Earth Observ. Remote Sens.*, vol. 9, no. 5, pp. 1854–1863, May 2016.
- [53] Code for Transport Planning on Urban Road (GB 50220–95), Ministry of Construction of the People's Republic of China, Beijing, China, 1995.
- [54] K. McGarigal and B. J. Marks, "Spatial pattern analysis program for quantifying landscape structure," US Dept. Agriculture, Forest Service, Pac. Northwest Res. Station, Portland, OR, USA, Gen. Tech. Rep. PNW-GTR-351, 1995.
- [55] Q. Luan, C. Ye, and W. Li, "Vegetation landscape change analysis based on remote sensing in northwest of Beijing," in *Proc. 21st Int. Conf. Geoinformat.*, 2013, pp. 1–6.
- [56] K. H. Riitters *et al.*, "A factor analysis of landscape pattern and structure metrics," *Landscape Ecol.*, vol. 10, no. 1, pp. 23–39, 1995.
- [57] P. S. Thenkabail, I. Mariotto, M. K. Gumma, E. M. Middleton, D. R. Landis, and K. F. Huemmrich, "Selection of hyperspectral narrowbands (HNBS) and composition of hyperspectral twoband vegetation indices (HVIs) for biophysical characterization and discrimination of crop types using field reflectance and Hyperion/EO-1 data," *IEEE J. Sel. Topics Appl. Earth Observ. Remote Sens.*, vol. 6, no. 2, pp. 427–439, Apr. 2013.
- [58] R. Dinuls, G. Erins, A. Lorencs, I. Mednieks, and J. Sinica-Sinavskis, "Tree species identification in mixed Baltic forest using LiDAR and multispectral data," *IEEE J. Sel. Topics Appl. Earth Observ. Remote Sens.*, vol. 5, no. 2, pp. 594–603, Apr. 2012.
- [59] B. Somers and G. P. Asner, "Invasive species mapping in Hawaiian rainforests using multi-temporal Hyperion spaceborne imaging spectroscopy," *IEEE J. Sel. Topics Appl. Earth Observ. Remote Sens.*, vol. 6, no. 2, pp. 351–359, Apr. 2013.
- [60] H. Zhao, P. Xiao, and X. Feng, "Edge detection of street trees in high-resolution remote sensing images using spectrum features," in *Proc. 8th Int. Symp. Multispectral Image Process. Pattern Recog.*, 2013, pp. 89180M-1–89180M-6.
- [61] M. F. Goodchild, "Citizens as sensors: The world of volunteered geography," *GeoJournal*, vol. 69, no. 4, pp. 211–221, 2007.



**Dawei Wen** received the B.S. degree in 2013 in surveying and mapping from Wuhan University, Wuhan, China, where she is currently working toward the Ph.D. degree in photogrammetry and remote sensing in the State Key Laboratory of Information Engineering in Surveying, Mapping, and Remote Sensing.

Her research interests include change analysis of multitemporal remote sensing images and remote sensing applications.



**Xin Huang** (M'13–SM'14) received the Ph.D. degree in photogrammetry and remote sensing in 2009 from Wuhan University, Wuhan, China, working with the State Key Laboratory of Information Engineering in Surveying, Mapping and Remote Sensing (LIESMARS).

He is currently a Full Professor with Wuhan University, Wuhan, China, where he teaches remote sensing, photogrammetry, image interpretation, etc. He is the Founder and Director of the Institute of Remote Sensing Information Processing (IRSIP), School of

Remote Sensing and Information Engineering, Wuhan University. He has published more than 80 peer-reviewed articles in the international journals. His research interests include hyperspectral data analysis, high-resolution image processing, pattern recognition, and remote sensing applications.

Prof. Huang was the recipient of the Top-Ten Academic Star of Wuhan University in 2009, the Boeing Award for the Best Paper in Image Analysis and Interpretation from the American Society for Photogrammetry and Remote Sensing (ASPRS) in 2010, the New Century Excellent Talents in University from the Ministry of Education of China in 2011, the National Excellent Doctoral Dissertation Award of China in 2012, and the China National Science Fund for Excellent Young Scholars in 2015. In 2011, he was recognized by the IEEE Geoscience and Remote Sensing Society (GRSS) as the Best Reviewer of IEEE GEOSCIENCE AND REMOTE SENSING LETTERS. He was the winner of the IEEE GRSS 2014 Data Fusion Contest. Prof. Huang was the lead guest editor of the special issue on information extraction from high-spatial-resolution optical remotely sensed imagery for the IEEE JOURNAL OF SELECTED TOPICS IN APPLIED EARTH OBSERVATIONS AND REMOTE SENSING (vol. 8, no.5, May 2015), and the lead guest editor of the special issue on Sparsity-Driven High Dimensional Remote Sensing Image Processing and Analysis for the Journal of Applied Remote Sensing (vol.10, no.4, Oct 2016). Since 2016, he serves as an Associate Editor of the Photogrammetric Engineering and Remote Sensing (PE&RS). Since 2014, he serves as an Associate Editor of the IEEE GEOSCIENCE AND REMOTE SENSING LETTERS.



**Hui Liu** received the B.S. degree in 2012 in mathematics from Wuhan University, Wuhan, China, where he is currently working toward the Ph.D. degree in the State Key Laboratory of Information Engineering in Surveying, Mapping, and Remote Sensing.

His research interests include image processing, object recognition, and remote sensing applications.



**Wenzhi Liao** (M'14) received the B.S. degree in mathematics from the Hainan Normal University, Haikou, China, in 2006, the Ph.D. degree in engineering from the South China University of Technology, Guangzhou, China, in 2012, and the Ph.D. degree in computer science engineering from Ghent University, Ghent, Belgium, in 2012.

Since 2012, he has been working as a Postdoctoral Researcher at Ghent University. His current research interests include pattern recognition, remote sensing, and image processing. In particular, his research inter-

ests include mathematical morphology, multitask feature learning, multisensor data fusion, and hyperspectral image restoration.

Dr. Liao is a member of the Geoscience and Remote Sensing Society (GRSS) and IEEE GRSS Data Fusion Technical Committee. He received the “Best Paper Challenge” Awards on both the 2013 IEEE GRSS Data Fusion Contest and the 2014 IEEE GRSS Data Fusion Contest.



**Liangpei Zhang** (M'06–SM'08) received the B.S. degree in physics from the Hunan Normal University, Changsha, China, in 1982, the M.S. degree in optics from the Chinese Academy of Sciences, Xian, China, in 1988, and the Ph.D. degree in photogrammetry and remote sensing from Wuhan University, Wuhan, China, in 1998.

He is currently the Head of the Remote Sensing Division, State Key Laboratory of Information Engineering in Surveying, Mapping and Remote Sensing, Wuhan University. He is also a Chang-Jiang Scholar

Chair Professor appointed by the Ministry of Education of China. He is currently a Principal Scientist for the China State Key Basic Research Project (2011–2016) appointed by the Ministry of National Science and Technology of China to lead the remote sensing program in China. He has more than 300 research papers. He is the holder of five patents. His research interests include hyperspectral remote sensing, high-resolution remote sensing, image processing, and artificial intelligence.

Dr. Zhang is a Fellow of the Institution of Engineering and Technology, an Executive Member (Board of Governor) of the China National Committee of the International Geosphere-Biosphere Programme, and an Executive Member of the China Society of Image and Graphics. He regularly serves as a Cochair of the series SPIE Conferences on Multispectral Image Processing and Pattern Recognition, Conference on Asia Remote Sensing, and many other conferences. He edits several conference proceedings, issues, and geoinformatics symposiums. He also serves as an Associate Editor of the *International Journal of Ambient Computing and Intelligence*, the *International Journal of Digital Multimedia Broadcasting*, the *Journal of Geo-spatial Information Science*, the *Journal of Remote Sensing*, and the IEEE TRANSACTIONS ON GEOSCIENCE AND REMOTE SENSING.